



## Previously unreported optical emissions generated during ionospheric heating

C. K. Mutiso,<sup>1</sup> J. M. Hughes,<sup>1</sup> G. G. Sivjee,<sup>1</sup> T. Pedersen,<sup>2</sup> B. Gustavsson,<sup>3</sup> and M. J. Kosch<sup>4</sup>

Received 2 May 2008; revised 22 May 2008; accepted 11 June 2008; published 19 July 2008.

[1] Several radio-induced optical emissions were generated during an ionospheric heating experiment performed at the High Power Auroral Stimulation (HIPAS) facility near Two Rivers, Alaska. The  $O^+$  732–733 nm and  $O(^3D^o)$  799.0 nm emissions, previously unreported from ionospheric heating experiments, were detected, in addition to the already documented  $O(^3P)$  844.6 nm and  $O(^5P)$  777.4 nm emissions. Maximum emission intensity was observed in the magnetic zenith, when the heater was transmitting continuous wave O-mode, at a frequency of 2.85 MHz. A modified Czerny-Turner grating spectrometer was used to acquire high resolution optical spectra of the induced emissions, which were synchronized to the heater duty cycle. Candidate mechanisms for the production of the radio-induced emissions, which occurred before the “double resonance” condition, are presented. **Citation:** Mutiso, C. K., J. M. Hughes, G. G. Sivjee, T. Pedersen, B. Gustavsson, and M. J. Kosch (2008), Previously unreported optical emissions generated during ionospheric heating, *Geophys. Res. Lett.*, 35, L14103, doi:10.1029/2008GL034563.

### 1. Introduction

[2] Ionospheric modification experiments leading to the production of radio-induced optical emissions (RIOEs) are now in their fourth decade. The pioneering observational efforts by *Sipler and Biondi* [1972], *Haslett and Megill* [1974], and *Gordon and Carlson* [1974] at low and mid-latitudes and *Brändström et al.* [1999], *Kosch et al.* [2000], *Pedersen and Carlson* [2001], and others at high latitudes are now well augmented by theory and modeling [e.g., *Bernhardt et al.*, 1989; *Istomin and Leyser*, 1995; *Mishin et al.*, 2004; *Gustavsson et al.*, 2005]. It is generally accepted that wave-particle interactions accelerate electrons which excite neutral (or ionized) constituents of the *E* and *F* region ionosphere, leading to the production of RIOEs.

[3] Until recently, observations of RIOEs were almost exclusively limited to the “forbidden”  $O(^1D)$  630.0 nm and  $O(^1S)$  557.7 nm transitions of atomic oxygen. The  $O(^1D)$ , with a relatively low excitation energy of 1.96 eV, is not strongly quenched in the *F* region and is the most commonly observed emission. Similarly, the  $O(^1S)$  557.7 nm

emission, with an excitation energy of 4.2 eV, is also readily observed in most experiments. However, collisional quenching of accelerated electrons by  $N_2$  in the *F* region raises the effective excitation thresholds of the  $O(^1D)$  and  $O(^1S)$  states to  $\sim 3.1$  and  $\sim 5.4$  eV, respectively [*Bernhardt et al.*, 1989].

[4] *Kosch et al.* [2000] first noted that, even for vertical heating, the optical emitting region was displaced toward the magnetic zenith. Later work by, for example, *Pedersen et al.* [2003], determined that the brightest emission intensity at high latitudes was in the magnetic zenith direction. These factors, coupled with significant improvements in detector technology, substantial increases in heater power, and favorable solar cycle conditions, have led to the detection of several higher-energy optical emissions. These include:  $O(^5P)$  777.4 nm (excitation energy 10.74 eV) [*Djuth et al.*, 2005],  $O(^3P)$  844.6 nm (10.99 eV) [*Gustavsson et al.*, 2005], and  $N_2^+$  427.8 nm (18.75 eV) [*Holma et al.*, 2006; *Gustavsson et al.*, 2006]. The detection of these emissions indicates electron acceleration to suprathermal energies. A thermal interpretation would require excessively high electron temperatures in order to produce these relatively higher-energy emissions [*Gustavsson et al.*, 2002].

[5] We present here observations of two previously unreported RIOEs: the  $O^+$  732–733 nm emission, with an excitation energy of 1.69–18.61 eV, depending on the excitation mechanism, and the  $O(^3D^o)$  799.0 nm emission, which has an excitation energy of 12.49 eV. Also observed during this experiment were the already documented  $O(^3P)$  844.6 nm and  $O(^5P)$  777.4 nm RIOEs.

### 2. Experiment Details

[6] The High Power Auroral Stimulation (HIPAS) optical campaign was carried out from 7–20 March 2007, at the HIPAS facility near Two Rivers, Alaska (64.9°N, 146.8°W). Observations presented here were obtained during the night of 19 March 2007, under clear skies. Geomagnetic conditions were quiet: *Kp* for this period was 1– and 0+; for the previous 24 hours *Kp*  $\leq$  1+. Absorption was negligible, as evinced by double-hop echoes on ionospheric sounding profiles. During the period of brightest optical emissions,  $f_oF_2$  was  $\sim 3.5$  MHz. The heater was transmitting O-mode, at a frequency of 2.85 MHz. This pump frequency was approximately equal to the local 2nd electron gyroharmonic ( $2f_{ce}$ ) at *F* region heights. As noted by *Kosch et al.* [2005], radio-induced optical emissions maximize near  $2f_{ce}$ , while minimizing at higher gyroharmonics. Starting at 0424 UT (2024 local time), the heater ran in a 6 min cycle: 50 ms pulses every 4 s for 2 min pointed above Poker Flat Research Range (dip angle  $\chi = 13^\circ$ , azimuth = 246°),

<sup>1</sup>Space Physics Research Laboratory, Embry-Riddle Aeronautical University, Daytona Beach, Florida, USA.

<sup>2</sup>Space Vehicles Directorate, Air Force Research Laboratory, Hanscom AFB, Bedford, Massachusetts, USA.

<sup>3</sup>Department of Physics and Technology, University of Tromsø, Tromsø, Norway.

<sup>4</sup>Communication Systems, Lancaster University, Lancaster, UK.

2 min of continuous wave, up-**B** (field-aligned) over HIPAS ( $\chi = 13^\circ$ , azimuth =  $204^\circ$ ), followed by 2 min off. When heating up-**B** over HIPAS, the total transmitter power was 588 kW; an antenna gain of 17.39 dB yielded an effective radiated power (ERP) of 32 MW.

[7] Optical measurements were obtained using a  $12^\circ$  circular field of view,  $f/4.5$ , modified Czerny-Turner grating spectrometer, consisting of: an order sorting filter; a 45 mm arc-length, 0.5 mm wide curved slit; a 0.5 m focal length spherical mirror; a  $110 \times 110$  mm, 1200 grooves/mm plane diffraction grating, blazed at 1000 nm; and a near-infrared optimized CCD camera with  $1024 \times 256$ ,  $26 \mu\text{m}$  square pixels. Light was focused onto the CCD chip by an  $f/1.4$ , 85 mm focal length compound lens. The CCD chip was cooled to  $-110^\circ\text{C}$ , significantly reducing the dark current, and leading to high signal-to-noise (S/N) ratios. Other diagnostics present for different periods of the campaign included several 630.0 nm and 557.7 nm imagers, and a Digisonde located at College, Alaska ( $\sim 50$  km away). Radar coverage was provided by the Kodiak SuperDARN HF radar and the Poker Flat Research Range (PFRR) Advanced Modular Incoherent Scatter Radar (AMISR).

### 3. Results

[8] Figure 1 shows sample spectra recorded by the spectrometer. As previously noted, each heater on or off period was 2 min long; however, the corresponding CCD scan time was shortened by 15 s in order to permit image read-out at the slowest possible rate. This significantly reduced the associated read-out noise and improved the S/N ratio. The free spectral range of the instrument was  $\sim 180$  nm, and the wavelength-dependent full width half maximum (FWHM) was 0.6–2 nm. The resolution at higher wavelengths was impaired by a focusing problem with the CCD lens. Prominent emission features in Figure 1a include the OH Meinel (8, 3), (9, 4), (5, 1) and (6, 2) bands starting at 727, 775, 791, and 834 nm respectively. Also visible are the  $\text{O}_2$  Atm. (0, 0) band centered at 762 nm, and the  $\text{O}_2$  Atm. (0, 1) band at 859 nm. The solid spectrum is an average of 3 consecutive up-**B** scans over HIPAS at 0544, 0550, and 0556 UT, while the dotted spectrum is an average of 3 consecutive heater off scans (0546, 0552, and 0558 UT). It should be noted that the heater-induced  $\text{O}^+$  and O emissions underlie brighter spectral features and are not discernible from Figure 1a alone. The difference in brightness between the on and off spectra in Figure 1a is not a heater-induced effect but is simply a changing background caused by the setting Sun.

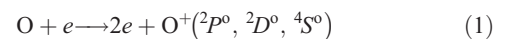
[9] Figures 1b–1d show background-subtracted, calibrated difference spectra in 10 nm bins surrounding the  $\text{O}^+$  732–733 nm, the  $\text{O}({}^5P)$  777.4 nm, and the  $\text{O}({}^3P)$  844.6 nm emissions. The difference spectra were obtained by subtracting the off spectrum from the on spectrum, and applying a background correction for each bin. The observed brightness is in R/nm, and the 777.4 nm and the 844.6 nm values agree well with the results of *Djuth et al.* [2005] and *Gustavsson et al.* [2005], respectively. The  $3\sigma$  standard deviation of the signal (99.7% confidence level) for each bin is shown as a horizontal dashed line. The emission peaks clearly stand out above the noise level.

[10] Figure 2 further illustrates the presence of RIOEs. Figure 2a is a time series of the ionospheric critical frequency,  $f_oF_2$ . The horizontal dashed line denotes the heater pump frequency,  $f_h$ , and the 2nd gyroharmonic,  $2f_{ce}$ , at 2.85 MHz. Pluses and diamonds in Figure 2b mark the altitudes of the plasma resonance layer (PRL) and the upper hybrid resonance layer (UHRL), respectively. The PRL corresponds to the altitude at which the plasma frequency,  $f_p$ , matches the heater frequency. At this altitude, the pump wave is reflected downward. The UHRL, which on average was 12 km below the PRL, is the altitude where upper hybrid waves [e.g., *Hughes et al.*, 2003] are generated. These waves, with a frequency  $f_{uh} = (f_p^2 + f_{ce}^2)^{1/2}$ , are intimately associated with many ionospheric heating phenomena [e.g., *Istomin and Leyser*, 1995; *Mishin et al.*, 2005], and are central in the production of heater-induced accelerated electrons [*Kosch et al.*, 2002]. Also shown in Figure 2b is the 2nd gyroharmonic altitude at  $\sim 245$  km, as determined from the IGRF 10 model. The shadow height is demarcated by the diagonal line. The vertical lines 1 and 2 mark the plasma resonance and “double resonance” conditions, respectively. Both are discussed below.

[11] Time series of background-subtracted, normalized optical intensities, plotted in conjunction with the heater duty cycle are presented in Figures 2c–2g. Heating pulses above PFRR are not included. The airglow intensity during each heater on and off period is divided by the intensity during the off period, yielding a ratio  $R_i$ , which for enhanced emissions is  $>1$  during the on periods, and is always 1 during the off periods. The degree of “correlation” between the heater and the emission enhancement is obtained by calculating the quantity  $C = \Sigma(R_i - 1)$ , summing over all the on and off periods. Clearly, an unenhanced emission has  $R_i \simeq 1$  and thus  $C \approx 0$ . Conversely, an emission modulated by the heater would be expected to have  $R_i > 1$ , and  $C > 0$ , the magnitude of  $C$  depending on the extent of the modulation. For this experiment, the  $\text{O}({}^3P)$  844.6 nm and the  $\text{O}({}^5P)$  777.4 emissions (Figures 2c–2d) show the highest correlation. The  $\text{O}^+$  732–733 nm and the  $\text{O}({}^3D^o)$  799.0 nm (Figures 2e–2f) display a somewhat weaker correlation, but modulation by the heater is still evident. Lastly, the  $\text{P}_1(2)$  line of the OH(9, 4) band at 779.4 nm (Figure 2g) shows a very low correlation and a lack of modulation by the heater.

### 4. Discussion

[12] The heater-induced  $\text{O}^+$  732–733 nm and  $\text{O}({}^3D^o)$  799.0 nm emissions are discussed here. The metastable  $\text{O}^+$  732–733 nm multiplet emission arises from the  $\text{O}^+({}^2P^o) \rightarrow \text{O}^+({}^2D^o)$  transition [*Sivjee et al.*, 1979]. Under auroral conditions, the  $({}^2P^o)$  state, together with the  $({}^2D^o)$  and the (ground)  $({}^4S^o)$  states are produced according to equation (1) in fractions of 0.2, 0.4 and 0.4, and requiring 18.61, 16.92, and 13.61 eV respectively [*Rees*, 1989].



[13] Photoionization gives rise to the emission in the twilight airglow spectrum [*Meriwether et al.*, 1978], and given the position of the terminator in Figure 2b, it is

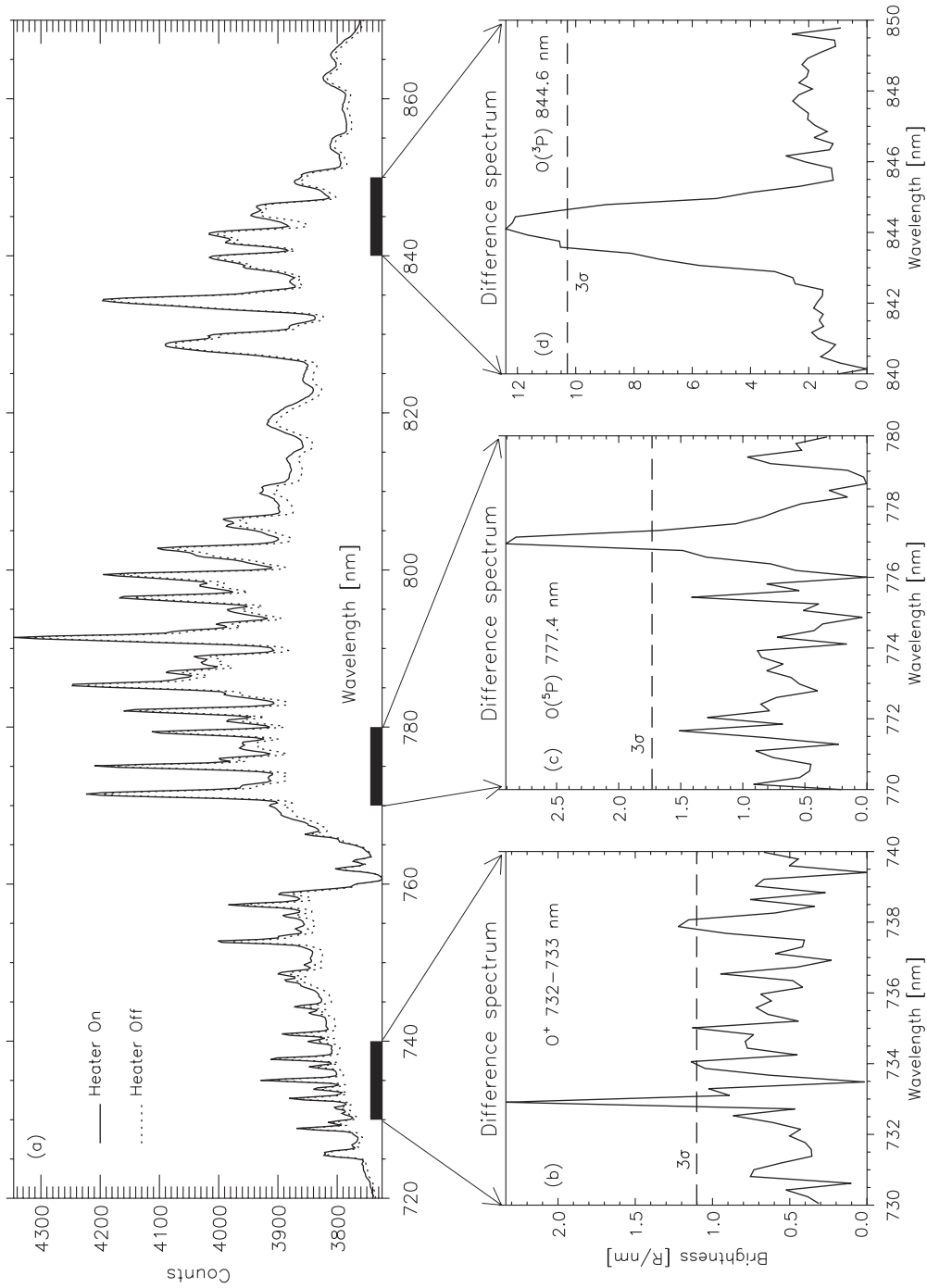


**Figure 1.** Airglow emissions recorded at HIPAS. (a) Sample spectra obtained during heater on (solid line) and heater off (dotted line) periods. Radio-induced optical emissions discussed in the text underlie brighter spectral features in the highlighted ranges. (b)–(d) Background-subtracted, calibrated difference spectra, showing radio-induced optical emissions at selected regions of interest.

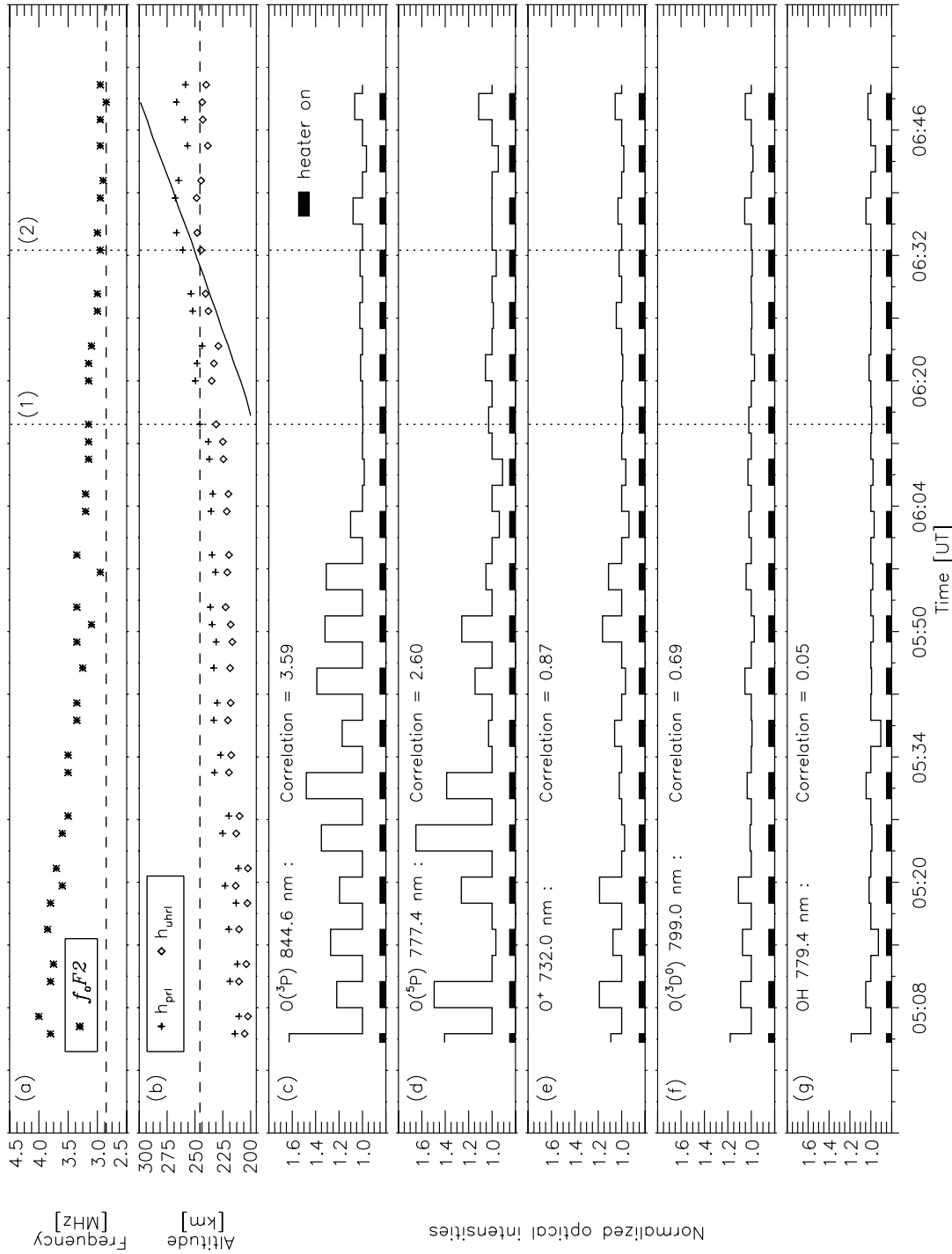


**Figure 2.** Ionospheric parameters and optical emission time series for 19 March 2007. (a) The ionospheric critical frequency,  $f_oF_2$ , derived from a Digisonde. The horizontal dashed line denotes the heater pump frequency and the 2nd gyroharmonic ( $2f_{ce}$ ), at 2.85 MHz. (b) Altitudes of the plasma resonance layer (+) and the upper hybrid resonance layer (◇). The horizontal line at  $\sim 245$  km indicates the 2nd gyroharmonic altitude. The diagonal line demarcates the shadow height. The vertical lines (1) and (2) correspond to the plasma resonance ( $\sim 0613$  UT) and the double resonance ( $\sim 0633$  UT) conditions respectively. (c)–(g) Background-subtracted, normalized optical intensities for various emissions plotted in conjunction with the heater duty cycle. The time series are normalized by dividing the emission intensity during the heater on and off periods by the intensity during the heater off period, for each pump cycle. The degree of “correlation” (see text for details) is also given.

apparent that our observed emissions were obtained from above the shadow height. Nevertheless, the data presented in Figures 2c–2f show clear modulations by the heater. Furthermore, twilight conditions produce suprathermal photoelectrons, and consequently, larger numbers of already energetic electrons are available for acceleration than is possible with a Maxwellian distribution. We therefore propose that either (or both) of  $O^+(^4S^o) \rightarrow O^+(^2P^o)$  (requiring 5.00 eV) or  $O^+(^2D^o) \rightarrow O^+(^2P^o)$  (1.69 eV) was caused by heater-induced electron acceleration and subsequent impact excitation of  $O^+$ . The reaction  $O + e \rightarrow 2e + O^+(^2P^o)$  (18.61 eV) cannot be ruled out, since *Gustavsson et al.* [2006] and *Holma et al.* [2006] have both observed heater-induced  $N_2^+$  427.8 nm (18.75 eV).

[14] The  $O^+$  732–733 nm emission spectra can be contaminated by the  $P_1(2)$  and the  $P_2(3)$  lines of the OH(8, 3) band, and by auroral  $N_2$  1P (5, 3). The latter can be discounted on the basis that electron energies hard enough to produce  $N_2$  emissions would have led to markedly different spectra. In addition, a 630.0 nm imager with a detection threshold of 3.5 R acquired simultaneous airglow images which show no background aurora. Regarding possible OH contamination of the  $O^+$  732–733 nm, the  $P_1(2)$  line of the OH(9, 4) band at 779.4 nm shows no modulation by the heater (Figure 2g). Thus, we expect no heater-induced modulation of the  $P_1(2)$  and the  $P_2(3)$  lines of the OH(8, 3) band. More significantly, OH production peaks at  $\sim 87$  km, over 100 km lower than the interaction altitudes determined here. We can therefore safely assume negligible modulation by the heater, and hence no OH emissions should be present in the difference spectra.

[15] The 799.0 nm multiplet is a weak auroral emission generated by the  $O(^3D^o) \rightarrow O(^3P)$  transition. It contributes significantly via cascade excitation to the  $O(^3P)$  844.6 nm emission, and in bright aurora its intensity is  $\sim 1\%$  of the  $O(^1S)$  557.7 nm green line [*Christensen et al.*, 1983]. The only possible significant source of contamination for this emission is OH, which we have addressed above.

[16] *Djuth et al.* [2005], *Kosch et al.* [2005], *Mishin et al.* [2005], and *Kosch et al.* [2007], among others, have presented data showing significant increases in optical emission brightness when the plasma resonance (Figure 2b, vertical line 1,  $\sim 0613$  UT) and double resonance (vertical line 2,  $\sim 0633$  UT) conditions were met. At plasma resonance,  $f_p = 2f_{ce} = f_h$ . Similarly, the double resonance condition is satisfied when  $f_{uh} = 2f_{ce} = f_h$ , that is, when the heater frequency matches the second gyroharmonic, at the upper hybrid resonance altitude. It is noteworthy that neither of these effects were observed in this experiment; in fact, the brightest emissions occurred approximately 1 hr before the double resonance condition. Simultaneous 630.0 nm and 557.7 nm observations display the same behavior.

[17] Ionospheric parameters were obtained from hand-fitted ionograms, which introduces a  $\pm 10$  km uncertainty in calculated ionospheric altitudes [*Kosch et al.*, 2005]. Nevertheless, taking this uncertainty into account would shift the plasma resonance to 0550 UT at the earliest, and the double resonance to 0618 UT. This would still be later than the period of maximum optical response starting at  $\sim 0520$  UT. In addition, any uncertainty due to the geographic separation of the Digisonde and the heater ( $1^\circ$  longitude,  $\sim 85$  km at  $F$  region heights) is expected to be

less than the  $\pm 10$  km uncertainty introduced by the ionograms. This is because the observations were carried out during quiet geomagnetic conditions and close to the terminator passage, so to first order the density gradients should be following the Sun. Thus, an uncertainty of about 4 minutes in the ionospheric parameters can be attributed to the geographic separation of the heater and the Digisonde; this still puts the maximum optical emissions outside the plasma resonance-double resonance window.

[18] Given the pump frequency used and the timing of the emissions with respect to the various resonances, there are several candidate mechanisms that could have generated the observed RIOEs. Chiefly, the parametric decay of the pump wave into Langmuir (L) and ion acoustic (IA) waves,  $PDI_L$ , is a well-known occurrence that efficiently accelerates electrons via Langmuir turbulence [*Fejer*, 1979]. This mechanism has been theoretically predicted by *Gurevich et al.* [2002] for pumping outside the Spitz cone ( $\sim 7.5^\circ$  at HIPAS), and ample experimental evidence exists [e.g., *Kosch et al.*, 2007, and references therein]. Also plausible is that the parametric decay ( $PDI_{EB}$ ) of the pump wave into electron Bernstein waves (EB) and lower hybrid (LH) waves [e.g., *Mishin et al.*, 2005; *Kosch et al.*, 2007] was in effect. The likely presence of suprathermal photoelectrons would have enhanced the airglow production of both mechanisms.

[19] In conclusion, we have presented spectroscopic observations of the previously unreported  $O^+$  732–733 nm and  $O(^3D^o)$  799.0 nm radio-induced optical emissions. Other documented RIOEs were also observed. All the emissions were detected in the magnetic zenith during O-mode  $F$  region heating at 2.85 MHz, and they display moderate to strong synchronization with the heater duty cycle. The generation of the emissions before double resonance favors a  $PDI_L$  or  $PDI_{EB}$  interpretation.

[20] **Acknowledgments.** This research was supported by Embry-Riddle Internal grant ERAU13213. The authors gratefully acknowledge the HIPAS personnel for their assistance in performing this experiment.

## References

- Bernhardt, P., C. Tepley, and L. Duncan (1989), Airglow enhancements associated with plasma cavities formed during ionospheric heating experiments, *J. Geophys. Res.*, *84*, 9071–9092.
- Brändström, B. U. E., T. B. Leyser, Å. Steen, M. T. Rietveld, B. Gustavsson, T. Aso, and M. Ejiri (1999), Unambiguous evidence of HF pump-enhanced airglow at auroral latitudes, *Geophys. Res. Lett.*, *26*, 3561–3564.
- Christensen, A. B., G. G. Sivjee, and J. H. Hecht (1983), OI (7990 Å) emission and radiative entrapment of auroral EUV, *J. Geophys. Res.*, *88*, 4911–4917.
- Djuth, F. T., T. R. Pedersen, E. A. Gerken, P. A. Bernhardt, C. A. Selcher, W. A. Bristow, and M. J. Kosch (2005), Ionospheric modification at twice the electron cyclotron frequency, *Phys. Rev. Lett.*, *94*, 125001, doi:10.1103/PhysRevLett.94.125001.
- Fejer, J. (1979), Ionospheric modification and parametric instabilities, *Rev. Geophys.*, *17*, 135–153.
- Gordon, W. E., and H. C. Carlson Jr. (1974), Arecibo heating experiments, *Radio Sci.*, *9*, 1041–1047.
- Gurevich, A. V., K. P. Zybin, H. C. Carlson, and T. Pedersen (2002), Magnetic zenith effect in ionospheric modifications, *Phys. Lett. A*, *305*, 264–274.
- Gustavsson, B., B. U. E. Brändström, Å. Steen, T. Sergienko, T. B. Leyser, M. T. Rietveld, T. Aso, and M. Ejiri (2002), Nearly simultaneous images of HF-pump enhanced airglow at 6300 Å and 5577 Å, *Geophys. Res. Lett.*, *29*(24), 2220, doi:10.1029/2002GL015350.
- Gustavsson, B., et al. (2005), The electron distribution during HF pumping, a picture painted with all colors, *Ann. Geophys.*, *109*, 1747–1754.

- Gustavsson, B., T. B. Leyser, M. Kosch, M. T. Rietveld, Å. Steen, B. U. E. Brändström, and T. Aso (2006), Electron gyroharmonic effects in ionization and electron acceleration during high-frequency pumping in the ionosphere, *Phys. Rev. Lett.*, *97*, 195002, doi:10.1103/PhysRevLett.97.195002.
- Haslett, J. C., and L. R. Megill (1974), A model of the enhanced airglow excited by RF radiation, *Radio Sci.*, *9*, 1005–1019.
- Holma, H., K. U. Kaila, M. J. Kosch, and M. T. Rietveld (2006), Recognizing the blue emission in artificial aurora, *Adv. Space Res.*, *38*, 2653–2658.
- Hughes, J. M., W. A. Bristow, R. T. Parris, and E. Lundell (2003), Super-DARN observations of ionospheric heater-induced upper hybrid waves, *Geophys. Res. Lett.*, *30*(24), 2276, doi:10.1029/2003GL018772.
- Istomin, Y. N., and T. B. Leyser (1995), Parametric decay of an electromagnetic wave near electron cyclotron harmonics, *Phys. Plasmas*, *2*, 2084–2097.
- Kosch, M. J., M. T. Rietveld, T. Hagfors, and T. B. Leyser (2000), High-latitude HF induced airglow displaced equatorwards of the pump beam, *Geophys. Res. Lett.*, *27*, 2817–2820.
- Kosch, M. J., M. T. Rietveld, A. J. Kavanagh, C. Davis, T. K. Yeoman, F. Honary, and T. Hagfors (2002), High-latitude pump-induced optical emissions for frequencies close to the third electron gyro-harmonic, *Geophys. Res. Lett.*, *29*(23), 2112, doi:10.1029/2002GL015744.
- Kosch, M. J., T. Pedersen, J. Hughes, R. Marshall, E. Gerken, A. Senior, D. Sentman, M. McCarrick, and F. T. Djuth (2005), Artificial optical emissions at HAARP for pump frequencies near the third and second electron gyro-harmonic, *Ann. Geophys.*, *23*, 1585–1592.
- Kosch, M. J., T. Pedersen, E. Mishin, S. Oyama, J. Hughes, A. Senior, B. Watkins, and W. A. Bristow (2007), Coordinated optical and radar observations of ionospheric pumping for a frequency pass through the second electron gyroharmonic at HAARP, *J. Geophys. Res.*, *112*, A06325, doi:10.1029/2006JA012146.
- Meriwether, J. W., Jr., D. G. Torr, J. C. G. Walker, and A. O. Nier (1978), The  $O^+(\text{}^2P)$  emission at 7320-Å in twilight, *J. Geophys. Res.*, *83*, 3311–3319.
- Mishin, E. V., W. J. Burke, and T. Pedersen (2004), On the onset of HF-induced airglow at HAARP, *J. Geophys. Res.*, *109*, A02305, doi:10.1029/2003JA010205.
- Mishin, E. V., M. J. Kosch, T. Pedersen, and W. J. Burke (2005), HF-induced airglow at magnetic zenith: Thermal and parametric instabilities near electron gyroharmonics, *Geophys. Res. Lett.*, *32*, L23106, doi:10.1029/2005GL023864.
- Pedersen, T. R., and H. Carlson (2001), First observations of HF heater-produced airglow at the High Frequency Active Auroral Research Program facility: Thermal excitation and spatial structuring, *Radio Sci.*, *36*, 1013–1026.
- Pedersen, T. R., M. McCarrick, E. Gerken, C. Selcher, D. Sentman, H. C. Carlson, and A. Gurevich (2003), Magnetic zenith enhancement of HF radio-induced airglow production at HAARP, *Geophys. Res. Lett.*, *30*(4), 1169, doi:10.1029/2002GL016096.
- Rees, M. H. (1989), *Physics and Chemistry of the Upper Atmosphere*, Cambridge Univ. Press, Cambridge, U. K.
- Sipler, D. P., and M. A. Biondi (1972), Measurements of  $O(^1D)$  quenching rate in the F region, *J. Geophys. Res.*, *77*, 6202–6212.
- Sivjee, G. G., G. J. Romick, and M. H. Rees (1979), Intensity ratio and center wavelengths of [O II] (7320–7330 Å) line emissions, *Astrophys. J.*, *229*, 432–438.

B. Gustavsson, Department of Physics and Technology, University of Tromsø, N-9037 Tromsø, Norway. (bjorn.gustavsson@phys.uit.no)

J. M. Hughes, C. K. Mutiso, and G. G. Sivjee, Space Physics Research Laboratory, Embry-Riddle Aeronautical University, Daytona Beach, FL 32114, USA. (hughesj@erau.edu; mutisoc@sprl.db.erau.edu; sivjee@erau.edu)

M. J. Kosch, Communication Systems, Lancaster University, Lancaster LA1 4WA, UK. (m.kosch@lancaster.ac.uk)

T. Pedersen, Space Vehicles Directorate, Air Force Research Laboratory, Hanscom AFB, Bedford, MA 01731–3010, USA. (Todd.Pedersen@hanscom.af.mil)